ACS APPLIED MATERIALS & INTERFACES

Research Article

www.acsami.org

Study on the Pretreatment of Poly(ether ether ketone)/Multiwalled Carbon Nanotubes Composites through Environmentally Friendly Chemical Etching and Electrical Properties of the Chemically Metallized Composites

Tong Zhai,[†,‡] Lizhi Di,[§] and De'an Yang*[,†,‡]

[†]Key Laboratory of Advanced Ceramics and Machining Technology Ministry of Education, Tianjin University, Tianjin 300072, P. R. China

[‡]School of Materials Science and Engineering, Tianjin University, Tianjin 300072, P. R. China

[§]Tianjin Medical College, Tianjin 300222, P. R. China

ABSTRACT: The high-volume resistivity and surface resistance of poly(ether ether ketone)/multiwalled carbon nanotubes (PEEK/MWCNT) composites restrict their use in an electronic field. To decrease the volume resistivity and surface resistance, we metalized the composites by electroless plating. The composites and metal coatings were characterized by SEM, XPS, AFM, EDX, and XRD spectroscopy. The swelling ratio of the composites, volume resistivity of two-side-coated composites, sheet resistance of plated composites, and adhesion between the coating and PEEK/MWCNT were tested. The results are as follows. A high roughness and a small swelling ratio were obtained by swelling in 18 mol/L H_2SO_4 for 3 min. Most of the MWCNT on the surface were still wrapped with PEEK after swelling. To expose the MWCNT, an environmentally friendly and effective etchant (MnO_2−NaH_2PO_4−H_2SO_4) was used. After etching, not only were high roughness and partially exposed MWCNT obtained but also the percentage of hydrophilic groups on the surface was increased. A dense cauliflower-like Ni−P coating was produced, and the exposed MWCNT were embedded in the metal coating after electroless plating for 20 min. The coating exhibited an amorphous structure with a phosphorus content of 11.21 wt %. The volume resistivity of two-side-coated PEEK/MWCNT dropped sharply to 38 Ω·m after electroless plating for 5 min. The sheet resistance decreased with increasing the electroless-plating time, and it dropped to 0.88 Ω/square after electroless plating for 40 min. The adhesion of the coating reached the highest 5 B scale (ASTM D3359) and could even undergo the test 20 times.

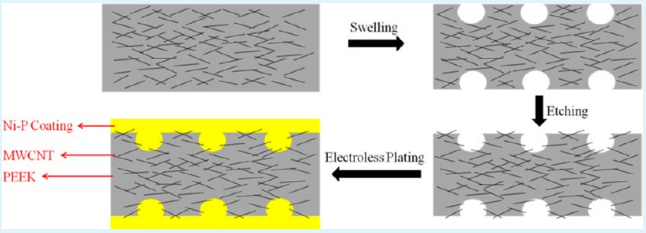

KEYWORDS: *PEEK/MWCNT composites, electroless plating, volume resistivity, sheet resistance, adhesion*

1. INTRODUCTION

The poly(ether ether ketone) (PEEK) polymer is a high-performance semicrystalline thermoplastic with outstanding features, such as superior mechanical properties[1] (Young's modulus, 4 GPa; tensile strength, 125 MPa), thermal stability[2] (glass transition temperature, 143 °C; melting point, 343 °C; onset of decomposition temperature, 580 °C), low flammability[3] (meeting Underwriters Laboratories 94V-0 requirements and having extremely low smoke emissions), radiation resistance[3] (1100 M γ radiation without significant degradation), and excellent chemical and hydrolysis resistance.[4,5] Because of these properties, it is widely used in the transportation (aircraft, aerospace, and automobiles) and energy industries, engineering applications, and medicine.

However, PEEK exhibits a high volume resistivity (10^{14} Ω·m) and surface resistance (10^{15} Ω).[6] This limits its use in the electronics field, where low resistivity of materials is required (such as in electromagnetic interference (EMI) shielding). Carbon nanotubes (CNT) are excellent candidates for the improvement of composites owing to their unique mechanical, electrical, and thermal properties combined with their small diameters and very low densities. Currently, lots of effort has been devoted to improving the properties of PEEK via incorporation with CNT. It has been reported that the incorporation of CNT into PEEK leads to an increase in mechanical properties, tribological properties, thermal stability, and thermal and electrical conductivity.[5] Wang et al.[6] reported that the volume resistivity and surface resistance of PEEK undergo a significant reduction by 9 orders of magnitude with the incorporation of 7 wt % multiwalled carbon nanotubes (MWCNT) and by 10 orders of magnitude with the incorporation of 12 wt % MWCNT. However, its volume resistivity and surface resistance were still much higher than metal and alloy (e.g., nickel, 1.0×10^{-7} Ω·m; electroless nickel,

Received: September 3, 2013
Accepted: November 12, 2013
Published: November 12, 2013

dx.doi.org/10.1021/am4037806 | *ACS Appl. Mater. Interfaces* 2013, 5, 12499−12509

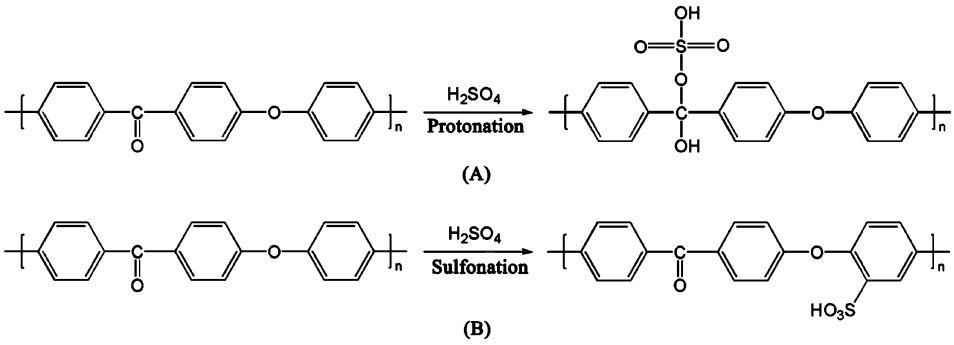

Figure 1. Reactions of protonation on the carbonyl groups (A) and sulfonation of PEEK (B).

5.6×10^{-7} Ω·m).[7] Although the average shielding effectiveness (SE) of PEEK with 12 wt % wrapped-MWCNT reached 50 dB in the 8−12 GHz frequency range, the average SE was only about 20 dB for frequencies lower than 8 GHz.[6] EMI consists of many unwanted radiated signals that can cause severe damage to communication systems and the safety operations of many electronic devices.[7] To prevent malfunctioning, electronic devices (especially in aircraft or spacecraft) must be shielded strictly. It has been reported that metals are excellent conductors of electricity and can absorb and reflect EMI.[7] To improve the electrical conductivity and EMI-shielding properties, it is necessary to metalize PEEK/MWCNT composites.

Conductive paints, electroplating, and electroless plating are the most common methods used for coating a metal layer on the surface of substrate materials. For conductive paints, the adhesion strength between the coating and substrate is weak. Electrodeposition is often used to deposit metal on the substrate with good conductivity. The materials with poor conductivity (such as PEEK and PEEK/MWCNT) cannot be metalized by using only the electrodeposition method because electrodeposition depends on an external source of direct current to reduce metallic ions in the electrolyte to metal on the substrate. Electroless plating is a chemical-reduction process that depends upon the catalytic reduction of a metallic ion in an aqueous solution containing a reducing agent. The driving force for these reactions arises from the potential difference that exists between the metal−solution interface and the equilibrium electrode potential for cathodic and anodic half-reactions.[8] Electroless nickel is widely used for engineering applications where excellent conductivity, uniform thickness, high hardness, wear resistance of the surface, and improved corrosion resistance are required.[9] For example, Guo et al. reported that SE values for Ni−P plated polyester fabric was about 50 dB in the frequency range of 10 MHz to 18 GHz.[10] Besides the above-mentioned advantages, the electroless-deposited film has another important function: it provides an electrically conductive substrate that allows for further coating by electroplating.

In this study, the surface of PEEK/MWCNT composites was chemically treated and metalized. It involves three main steps: (1) surface treatment, (2) surface activation, and (3) electroless metallization with nickel−phosphorus. Among them, the most critical step is the surface treatment. Because the surface of PEEK/MWCNT composite is hydrophobic and the surface activity with metal is low, the composite surface must be treated to obtain an excellent hydrophilicity for the adsorption of the metal Pd catalyst to initiate electroless plating and a high roughness for a mechanical anchorage of the coating to enhance adhesion. In recent years, several methods have been used for polymer surface treatment. Badyal et al.[11] used pulsed plasma to functionalize a poly(tetrafluoroethylene) surface, Piotr et al.[12] used an excimer laser for the surface treatment of polyamide composites, and Hvilsted et al.[13] used a chemical grafting method to modify a PEEK film. Considering the cost factor, the most common method is chemical etching. Until now, the best chemical-etching process has been based on chromic acid etching. However the presence of Cr^{6+} in chromic acid poses a serious environmental threat. In our work, we provided an environmentally friendly and cost-effective method to roughen and hydrophilize the surface of PEEK/MWCNT composites by swelling them in concentrated sulfuric acid and etching in a MnO_2−NaH_2PO_4−H_2SO_4 system. After treatment, the composites could be easily metalized, which results in a low volume and surface resistance. Additionally, we speculate that this pretreatment method will also be suitable for the metallization of other poly(aryl ether ketone)/CNT composites.

2. EXPERIMENTAL SECTION

2.1. Materials. Semicrystalline PEEK and PEEK/MWCNT composite were supplied by Jilin University. The content of MWCNT in the composite was 12 wt %. To produce amorphous PEEK, semicrystalline PEEK samples were heated at 390 °C and then quenched in ice water. The dimension of the samples used for electroless plating was 15 ×15 ×2 mm^3. The samples used for swelling-ratio measurements were disks (10 mm in diameter and 2 mm thick). All reagents used in this study were of an analytical pure reagent grade.

2.2. Methods. *2.2.1. Surface Treatment.* First, the PEEK/MWCNT and semicrystalline and amorphous PEEK samples were degreased in alkaline solution (NaOH 25 g/L, Na_2CO_3 40 g/L, Na_3PO_4 35 g/L, emulsifier OP-10 2 mL/L) at 60 °C for about 15 min followed by rinsing with water. The purpose of degreasing is to remove the oil stain on the surface of PEEK/MWCNT samples so that the uniformity of the swelling and etching process can be improved and the adhesive force between the coating and the substrate can be increased. Second, the swelling process was carried out with a swelling agent. The effect of H_2SO_4 concentration (12.6, 15.3, 16.5, and 18 mol/L) and swelling time (3, 6, 9, and 12 min) were investigated. In this process, PEEK was protonated by adding a proton H^+ to carbonyls in the main chain and sulfonated by replacing a hydrogen atom on phenyl ring with a sulfonic acid functional group. The reactions of protonation on the carbonyl groups and sulfonation of PEEK are shown in Figure 1. Because of the protonation and sulfonation, PEEK was partly dissolved in strong acids.[14] Third, the swelled samples were etched in an MnO_2−H_2SO_4 colloid system (10 g/L MnO_2 and 12.6 mol/L H_2SO_4) at 60 °C for 5 min and a MnO_2−NaH_2PO_4−H_2SO_4 colloid system (10 g/L MnO_2, 120 g/L $NaH_2PO_4{\cdot}2H_2O$, and 12.6 mol/L H_2SO_4) at 60 °C for different amounts of time to study the effect of NaH_2PO_4 on the etching process. Fourth, the etched samples were kept in a neutralizing solution ($H_2C_2O_4$ 20 g/L and H_2SO_4 1.8

mol/L) at 60 °C for 10 min to remove residual MnO_2. The reaction equation is as follows

$$MnO_2 + H_2C_2O_4 + 2H^+ \rightarrow Mn^{2+} + 2CO_2 + 2H_2O$$

To study the relationship between the phase composition and dissolution rate, amorphous and semicrystalline PEEK were put into 18 mol/L H_2SO_4 at room temperature for 6 min. After that, the swelled samples were rinsed thoroughly with deionized water to remove the residual H_2SO_4. Then, the samples were dried by placing them into oven at 140 °C.

2.2.2. Surface Activation. First, surface sensitization was conducted by immersing the treated samples into a sensitization bath ($SnCl_2 \cdot 2H_2O$ 22.5 g/L and HCl 0.6 mol/L) at room temperature for 20 min. The samples were subsequently rinsed with deionized water to remove excess stannous ion (Sn^{2+}). Then, the samples were activated through immersing into an activation bath ($PdCl_2$ 0.25 g/L and HCl 1.2 mol/L) at room temperature for 20 min. In this process, palladium ion (Pd^{2+}) was reduced by Sn^{2+} to Pd nuclei (Pd^0). The reaction equation is as follows

$$Pd^{2+} + Sn^{2+} \rightarrow Sn^{4+} + Pd^0\downarrow$$

The Pd nuclei tightly attached to the surface of the sensitized samples and acted as catalyst to initiate the electroless plating. After that, the samples were dipped into a reduction bath ($NaH_2PO_2 \cdot H_2O$ 25 g/L) at room temperature for 30 s to heighten the catalytic activity of the surface and to prevent the electroless plating bath from being contaminated.

2.2.3. Electroless Plating. The surface activated samples was placed in the homemade electroless nickel plating bath at pH 5.0. The samples were left in the bath at 60 °C for different amounts of time. The plating bath contained $NiSO_4 \cdot 6H_2O$ (25 g/L) as a source of Ni^{2+}, $NaH_2PO_2 \cdot H_2O$ (25 g/L) as a reducing agent, and $C_6H_8O_7 \cdot H_2O$ (25 g/L) as complexing agent. The pH of the plating bath was adjusted using an ammonia solution.

2.2.4. Electrodeposition. A big disadvantage of electroless plating is that the deposition rate is low and difficult to control. However, the electroplating technique can overcome this limitation. Some of the electroless-plated samples were electroplated in a nickel electroplating bath (pH 4.6) at 60 °C with a current density of 2.8 A/dm^2 for 20 min. The main components of the electroplating bath were $NiSO_4 \cdot 6H_2O$ (250 g/L), $NiCl_2 \cdot 6H_2O$ (30 g/L), and H_3BO_3 (40 g/L).

2.3. Characterization. The surface topographies of the PEEK/MWCNT samples and Ni−P coatings were observed by scanning electron microscopy (SEM, Hitachi S4800) equipped with a field-emission gun and coupled with an energy-dispersive X-ray spectrometer (EDX). The surface composition of the Ni−P coating was characterized by EDX. The surface composition and chemistry of the PEEK/MWCNT samples before and after treatment were determined by X-ray photoelectron spectroscopy spectra (XPS, PerkinElmer PHI-1600) equipped with a monochromatic Al Kα X-ray source. The analyzer's pass energy was set to 188 eV to record survey spectra and to 29 eV to take high-resolution spectra. PHI-MATLAB software was used to analyze the XPS spectra. The surface roughness of the PEEK/MWCNT substrates was measured by atomic force microscopy (AFM 5500, Agilent) and reported as average roughness (R_a) and root-mean-square roughness (R_{ms}). The structure of the PEEK, PEEK/MWCNT, and Ni−P coatings was analyzed by X-ray diffraction (XRD) using a Rigaku D/MAX-2500 diffractometer and Cu Kα radiation.

The dissolution rate (DR) was calculated according to the following equation

$$DR = \frac{W_1 - W_2}{S}$$

In this equation, W_1 and W_2 are the mass of the samples before swelling and after drying, respectively. S is the surface area of the semicrystalline and amorphous PEEK samples before swelling.

To study the impact of the swelling time on the PEEK/MWCNT composite and on semicrystalline PEEK, the extent of swelling for those samples was measured. The extent of swelling was calculated according to the following equation

$$SR = \frac{V_2 - V_1}{V_1} \times 100$$

In this equation, the swelling ratio (SR) represents the swelling extent. V_1 and V_2 are the volumes of the samples before and after swelling, respectively. V_1 and V_2 were measured by Archimedes method (suspension method).[15] The volume was calculated according to the following equation

$$V = \frac{M_1 - M_2}{\rho}$$

where ρ is the density of the liquid, M_1 and M_2 are the weights of the samples in air and liquid, respectively, and V is the unknown volume of the sample.

The sheet resistance of Ni−P coated PEEK/MWCNT samples was measured by the four-point probe method (SDY-5, China) at room temperature. The adhesion between the Ni−P coating and PEEK/MWCNT substrate was studied by the standard ASTM D3359 Scotch-tape test.[16,17] This test consists of applying and removing pressure-sensitive adhesive tape over 16 cross-hatched squares of 1 × 1 mm^2 made in the coating. With this method, the adhesion can be assessed qualitatively on the 0 to 5 B scale.

3. RESULTS AND DISCUSSION

3.1. Swelling. *3.1.1. Phase Composition and Dissolution Rate.* Figure 2 shows the XRD patterns of the as-received PEEK (A), quenched PEEK (B), and PEEK/MWCNT (C). In Figure 2A, the four main peaks at 18.8, 20.7, 22.9, and 28.9° correspond to the diffraction of the (110), (111), (200), and (211) crystalline planes of the PEEK, respectively, and the high background around 20° corresponds to the amorphous phase, so the as-received PEEK is semicrystalline. In Figure 2B, a single broad peak centered at 20° indicated the amorphous nature of the quenched PEEK. The measured dissolution rate was 3.18 mg/cm^2 for amorphous PEEK and 0.40 mg/cm^2 for semicrystalline PEEK. This demonstrated that the dissolution rate of the amorphous phase was greater than that of the crystalline phase. In amorphous regions, the molecular packing is loose, and the interaction force between molecules is weak, so solvent molecules can easily penetrate into the amorphous regions. However, in crystalline regions, molecules arrange regularly and pack tightly, and the interaction force between

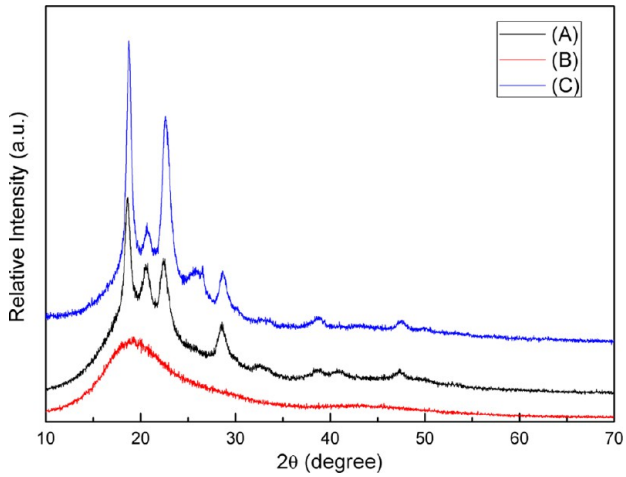

Figure 2. XRD patterns of the as-received PEEK (A), quenched PEEK (B), and PEEK/MWCNT (C).

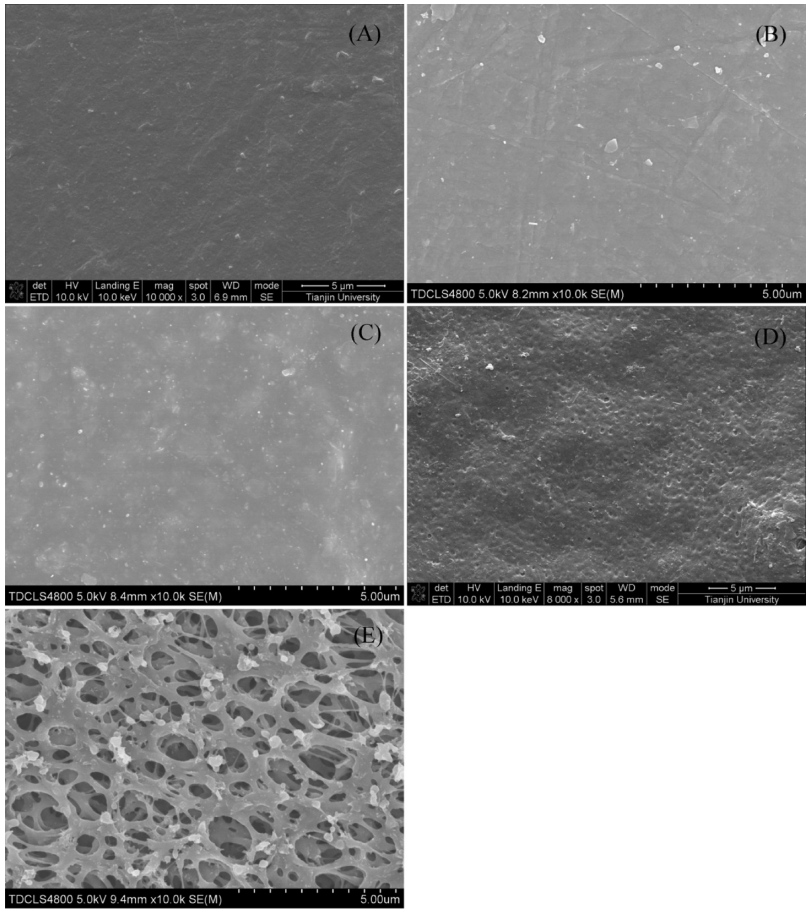

Figure 3. SEM images of PEEK/MWCNT samples before swelling (A) and after swelling in 12.6 mol/L H_2SO_4 (B), 15.3 mol/L H_2SO_4 (C), 16.5 mol/L H_2SO_4 (D), and 18 mol/L H_2SO_4 (E) for 3 min at room temperature.

molecules is strong, so it is difficult for solvent molecules to penetrate into the crystalline regions. Therefore, the dissolution rate of the amorphous phase is greater than that of the crystalline phase.

3.1.2. Surface Morphology. In our research, we used 12.6, 15.3, 16.5, and 18 mol/L H_2SO_4 as swelling agents, respectively. Figure 3 shows the surface morphology of the PEEK/MWCNT samples before and after swelling. As shown in Figure 3A, the surface of the PEEK/MWCNT samples was smooth and compact before swelling. No holes or flaws could be seen on the surface, and only some traces of mold were left on the surface. In Figure 3B, the surface morphology was nearly unchanged, and we could still see the traces of mold. That is to say, 12.6 mol/L H_2SO_4 had little effect on the surface of the PEEK/MWCNT composite. This result is in accord with the research of Bishop et al. who reported that PEEK powder was negligibly soluble in 14 mol/L H_2SO_4, partially soluble in 16 mol/L H_2SO_4, and completely soluble in 18 mol/L H_2SO_4.[14] After the samples were left in 15.3 mol/L H_2SO_4 for 3 min at room temperature (Figure 3C), the traces of mold disappeared. However, the surface was still smooth and compact. It is possible that the dissolution rate was rather low. In Figure 3D, nanosized holes appeared on the surface of the samples swelled in 16.5 mol/L H_2SO_4 for 3 min at room temperature. However the depth of the holes was too shallow, and the shape of the holes was opening, so efficient anchorage effect could not be formed. After the samples were left in 18 mol/L H_2SO_4 for 3 min at room temperature (Figure 3E), microscopic holes appeared on the surface. The XRD pattern (Figure 2C) shows the semicrystalline structure of PEEK in the composite. Because the dissolution rate of the amorphous phase is greater than that of the crystalline phase, holes were formed on the surface of the samples, as shown in Figure 3D,E.

3.1.3. Swelling Ratio. Figure 4 shows the SR values of semicrystalline PEEK and PEEK/MWCNT samples swelled in

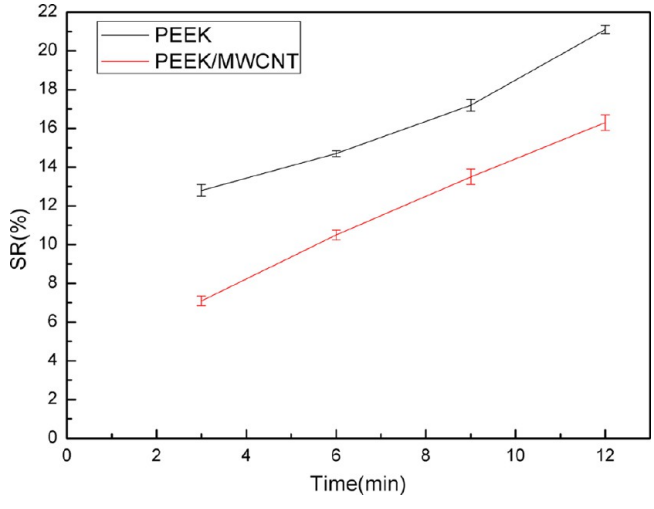

Figure 4. Swelling behavior of the PEEK/MWCNT composite and pure PEEK at different amounts of swelling time.

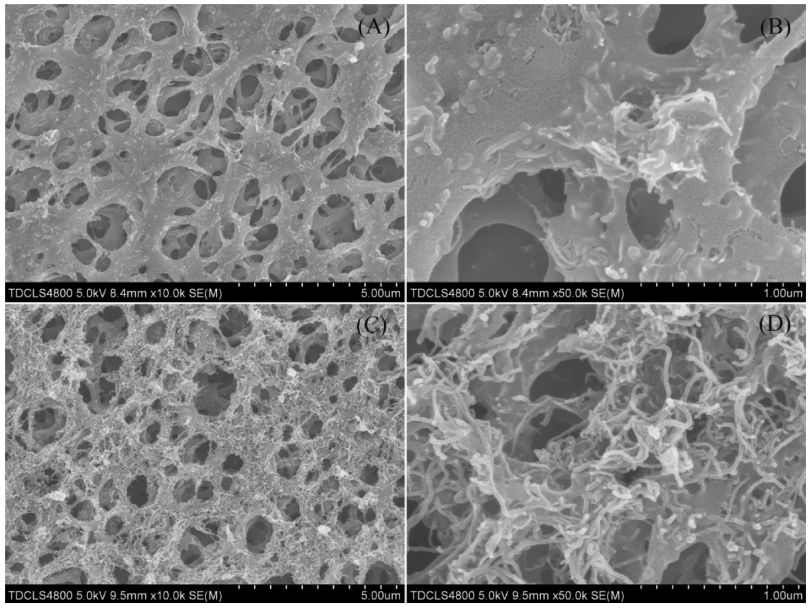

Figure 5. SEM images of the samples etched in the MnO_2–H_2SO_4 (A, B) and MnO_2–NaH_2PO_4–H_2SO_4 systems (C, D) for 5 min. Panel B is the same magnification as panel A, and panel D is the same magnification as panel C.

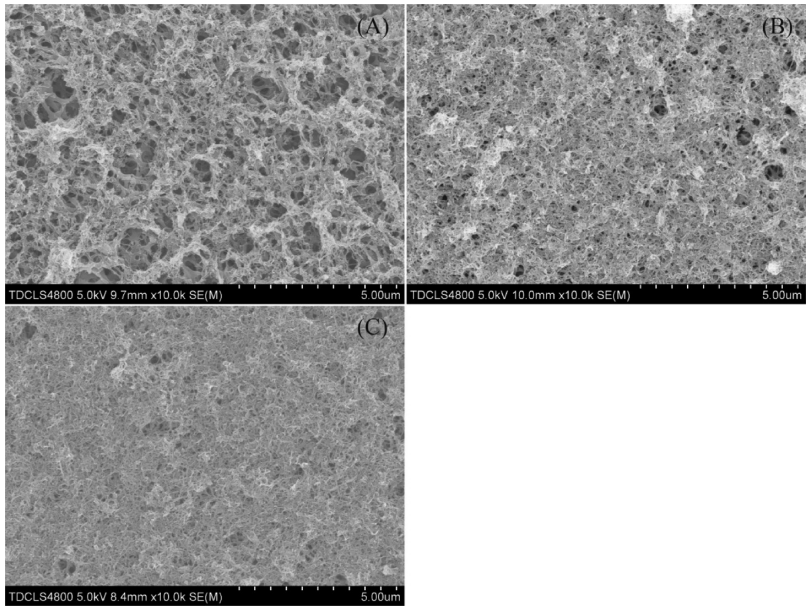

Figure 6. SEM images of the samples etched in the MnO_2–NaH_2PO_4–H_2SO_4 system for 10 (A), 20 (B), and 30 min (C).

18 mol/L H_2SO_4 at room temperature for different amounts of time (3, 6, 9, and 12 min). The SR of both the PEEK/MWCNT and PEEK samples increased with the increase of the swelling time. However, for the same swelling time, the SR of the PEEK/MWCNT composite was smaller than that of PEEK. For example, the SR of the PEEK/MWCNT composite swelled for 3 min was 7.1%, but the SR of PEEK was 12.8%. This demonstrated that the PEEK/MWCNT composite had good antiswelling properties. It has been reported that well-dispersed MWCNT form a network throughout the PEEK matrix.[5] In addition, there was an effective interfacial adhesion between PEEK and MWCNT. Both of these factors restrained the swelling of the PEEK/MWCNT samples and resulted in their good antiswelling capability. The antiswelling capability is important to electroless plating because the swelled PEEK shrink during the drying process of the plated samples. Thus, an interfacial stress is generated between the substrate and metal coating. A large interfacial stress will lead to the cracking or desquamating of the metal coating. Therefore, the SR should not be too large, and 3 min is a suitable swelling time.

3.2. Etching. Figure 5A,B shows the surface morphology of the samples etched in the MnO_2–H_2SO_4 system at 60 °C for 5 min. The surface still had many microscopic holes (Figure 5A), and the contours of MWCNT could be seen on the wall of the microscopic holes (Figure 5B). This is different from the morphology of the swelled samples in which the wall of the microscopic holes was smooth and hardly any MWCNT contours were exposed on the porous surface (Figure 3E). Figure 5C,D shows the surface morphology of the samples etched in the MnO_2–NaH_2PO_4–H_2SO_4 colloid system at 60

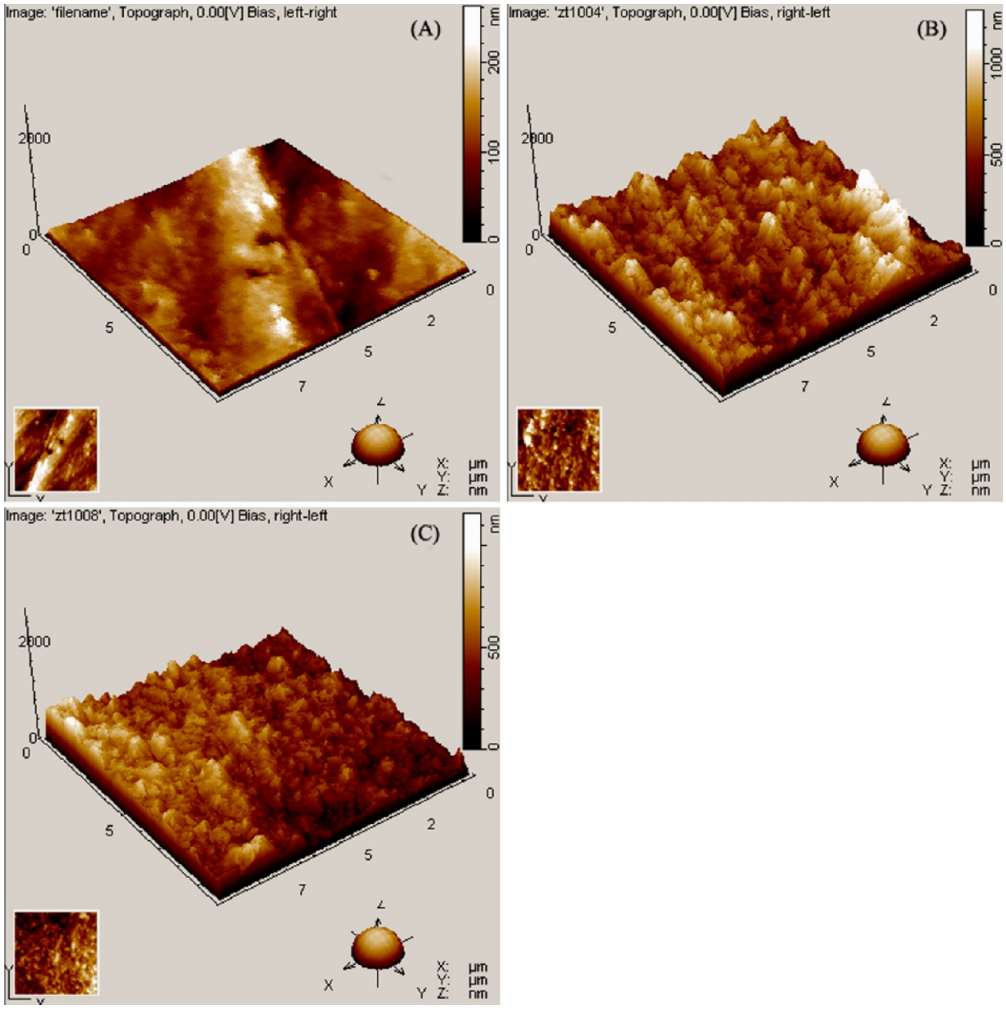

Figure 7. AFM images of the PEEK/MWCNT samples before (A) and after (B) swelling in 18 mol/L H_2SO_4 for 3 min at room temperature and after etching in the MnO_2–NaH_2PO_4–H_2SO_4 system at 60 °C for 5 min (C).

°C for 5 min. The surface still had lots of microscopic holes (Figure 5C), and many partially exposed MWCNT could be seen clearly (Figure 5D). By comparing Figure 5, panels D and B, the number of MWCNT per unit area using the MnO_2–NaH_2PO_4–H_2SO_4 system was larger than that by using the MnO_2–H_2SO_4 system. Because the oxidizability of the MnO_2–H_2SO_4 system is a little smaller than that of CrO_3–H_2SO_4,[18] the PEEK at the surface of the sample was oxidized and dissolved into the etching solution, so the contours of MWCNT appeared. When NaH_2PO_4 was added into the MnO_2–H_2SO_4 solution, it chelated Mn(IV) ions, and the content of soluble Mn(IV) in the etching solution increased. The etching process was a dynamic process, and the increase of the soluble Mn(IV) content in the colloid was conducive to the supplement of the oxidant in the etching process.[19] This is why lots of MWCNT were exposed after etching in the MnO_2–NaH_2PO_4–H_2SO_4 system. The exposed MWCNT could contact the Ni–P coating, and this is important for reducing the volume resistivity of the PEEK/MWCNT composite.

Figure 6A–C shows the surface morphology of the samples etched in the MnO_2–NaH_2PO_4–H_2SO_4 colloid system at 60 °C for 10, 20, and 30 min, respectively. It can be seen that the microscopic holes were destroyed after 10 min of etching, and they almost disappeared after 20 and 30 min of etching. The microscopic holes on the surface are important for the anchorage effect of the metal coating. In the following experiment, the samples were etched in the MnO_2–NaH_2PO_4–H_2SO_4 system at 60 °C for 5 min.

Because surface roughness is an important factor for the adhesion of the metal coating and the wettability of the substrate, the surface roughness of untreated, swelled, and etched PEEK/MWCNT samples was measured by AFM (Figure 7). The untreated PEEK/MWCNT surface exhibited a smooth topography (Figure 7A), and the values of R_a and R_{ms} were 61 and 76 nm, respectively. When the PEEK/MWCNT samples were swelled in 18 mol/L H_2SO_4 for 3 min at room temperature, the surface roughness increased significantly, as shown in Figure 7B. The R_a and R_{ms} values reached 151 and 196 nm, respectively. After etching in the MnO_2–NaH_2PO_4–H_2SO_4 system at 60 °C for 5 min (Figure 7C), the R_a and R_{ms} values slightly decreased to 140 and 175 nm, respectively. The roughness of the etched samples was a little smaller than that of the swelled samples because the PEEK at the surface was etched (indicated in Figure 5D). Compared with the reported roughness,[20] the high surface roughness of the etched samples guaranteed the presence of sufficient bonding sites for the deposited metal and increased the wettability of the substrate.

To obtain the surface composition changes of the samples before and after treatment, XPS analyses were undertaken. Typical XPS survey spectra (Figure 8) contain the characteristic

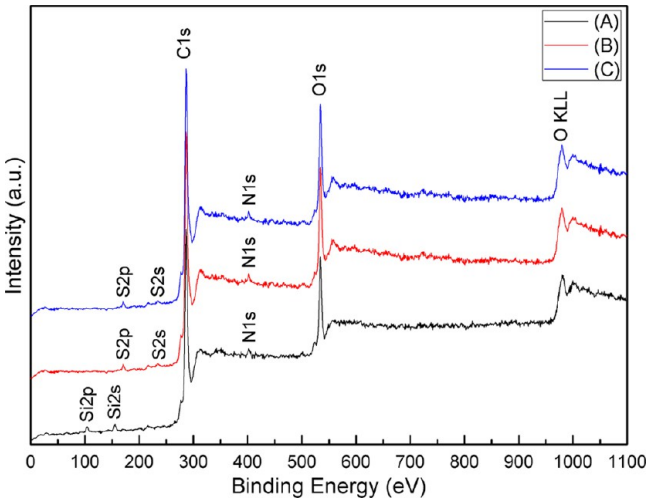

Figure 8. Typical XPS survey spectra of PEEK/MWCNT samples before swelling (A), after swelling in 18 mol/L H_2SO_4 (B), and after etching in the MnO_2–NaH_2PO_4–H_2SO_4 system (C).

peaks of C, O, Si, N, and S. Table 1 lists their atomic content (atom %) and the oxygen-to-carbon ratio (O/C). The nitrogen element might be introduced by MWCNT. The silicon element might be introduced by processing additives. A small amount of sulfur was detected after etching because of the protonation and sulfonation of PEEK by concentrated sulfuric acid. The O/C of the untreated PEEK/MWCNT samples (19.8%) is higher than the theoretical value of PEEK (15.8%). This might be caused by silicon-containing additives (such as silane coupling agents). After swelling, O/C was increased to 20.4%, and this can be attributed to $-OSO_3H$ and $-SO_3H$ groups created from the protonation and sulfonation of PEEK. Then, the O/C of the etched samples increased to 21.3%. This can be attributed to the oxidization of PEEK and MWCNT during chemical etching. It should be noted that lots of MWCNT were exposed after etching. The O content of MWCNT was lower than that of PEEK, and this will result in the decrease of O content on the etched surface. However, the O content was increased, so we deduced that MWCNT were also oxidized (discussed in detail in the analysis of high-resolution C 1s spectra).

Table 1. Surface Composition (atom %) and O/C (%) before Swelling, after Swelling, and after Etching

sample	C	O	Si	N	S	O/C
before swelling	79.9	15.8	2.8	1.6	0	19.8
after swelling	80.9	16.5	0	1.7	0.9	20.4
after etching	80.8	17.2	0	1.4	0.6	21.3

Oxidized groups carrying a distinct polarity were formed during the etching treatment. The effect of etching on the variation of surface functional groups can be extracted from the high-resolution C 1s spectra of the samples before swelling (Figure 9A), after swelling (Figure 9B), and after etching (Figure 9C). From Figure 9A, the C 1s spectrum of the untreated PEEK/MWCNT is the result of the contribution of five components: the C−C groups (phenyl and MWCNT) at a binding energy of 284.61 eV, the C−O groups (ether) at 286.23 eV, the C═O groups (carbonyl) at 288.46 eV, and two shakeup satellite peaks (aromatic structures in MWCNT and PEEK) at 290.13 and 291.69 eV. In Figure 9B, after swelling in 18 mol/L H_2SO_4 for 3 min at room temperature, the content of C−C groups (284.55 eV) decreased from 73.52 to 67.12%. The content of C−O groups (286.29 eV) increased from 21.68 to 25.23%, and the content of C═O groups (288.61 eV) decreased from 2.39 to 1.82%. This is because the carbonyl groups of PEEK were protonated after swelling, as shown in Figure 1A. Although the hydrophilic carbonyl group decreased, the hydrophilic hydroxyl (−OH) and sulfonic acid ($-SO_3H$) groups increased. In Figure 9C, after etching in the MnO_2–NaH_2PO_4–H_2SO_4 system at 60 °C for 5 min, the content of C−C groups (284.55 eV) decreased to 65.18%. The content of C−O groups (286.29 eV) was 24.57%. This is little smaller than swelled samples (25.23%), but it is still larger than untreated samples (21.68%). This may be the result of the following two factors. First, the percentage of PEEK was decreased after etching; thus, the content of C−O groups was reduced. Second, part of the C−O groups were oxidized to hydrophilic C═O or −COOH (carboxyl) groups. Apparently, the content of C═O groups (288.55 eV) increased from 1.82 (swelled sample) to 5.12%. This can be attributed to the oxidization of the etching solution, which can oxidize both PEEK and MWCNT. According to literature,[21] −COOH groups can be covalently bonded to CNT in a solution with acidity and oxidization, and the −COOH groups are at a binding energy of 288.39−289.54 eV. Therefore, we speculate that not only carbonyl groups but also carboxyl groups formed during the etching treatment. The hydroxyl, carbonyl, sulfonic acid, and carboxyl groups increased the hydrophilic character of the composite surface and consequently increased the absorption of Pd nuclei.

3.3. Metal Coating. The etched samples were activated and then put into the electroless nickel plating bath for metallization. Figure 10 shows the surface morphology of the samples after electroless plating for 30 s or for 2, 5, 10, and 20 min (corresponding to panels A−E, respectively). After plating for 30 s, Ni−P alloy nanoparticles began to deposit on the surface of PEEK/MWCNT, especially on the surface of MWCNT. After plating for 2 min, MWCNT were covered by Ni−P alloy completely, but there were many holes on the surface of the composite. The holes reduced gradually as the plating time increased. After plating for 20 min, the cavities disappeared completely, and the Ni−P coating exhibited a nodular structure that resembles the surface of cauliflower (Figure 10 E).

The Ni−P coating (electroless plating for 20 min) was analyzed by EDX (Figure 11) and XRD (Figure 12). From Figure 11, it was confirmed that the main elements of the coating included Ni and P and the content of phosphorus was 11.21 wt %. According to the literature,[9] the degree of corrosion resistance for a Ni−P coating is greatly affected by the phosphorus content, and alloys containing more than 10 wt % P are more resistant to attack than those with lower phosphorus content when in a neutral or acidic environment. Therefore, the coating on the surface of PEEK/MWCNT had a good corrosion resistance. For comparison, Figure 12 shows the XRD patterns of PEEK/MWCNT samples (A) and the Ni−P coating (B). In Figure 12B, the peaks in the range of 15−30° were assigned to PEEK/MWCNT substrate. The single broad peak centered at 45° indicated the amorphous nature of the Ni−P coating. The structural peculiarities of amorphous alloys lead to unique mechanical and physical properties such as soft magnetism, high tensile strength and elasticity, and high corrosion resistance.[22]

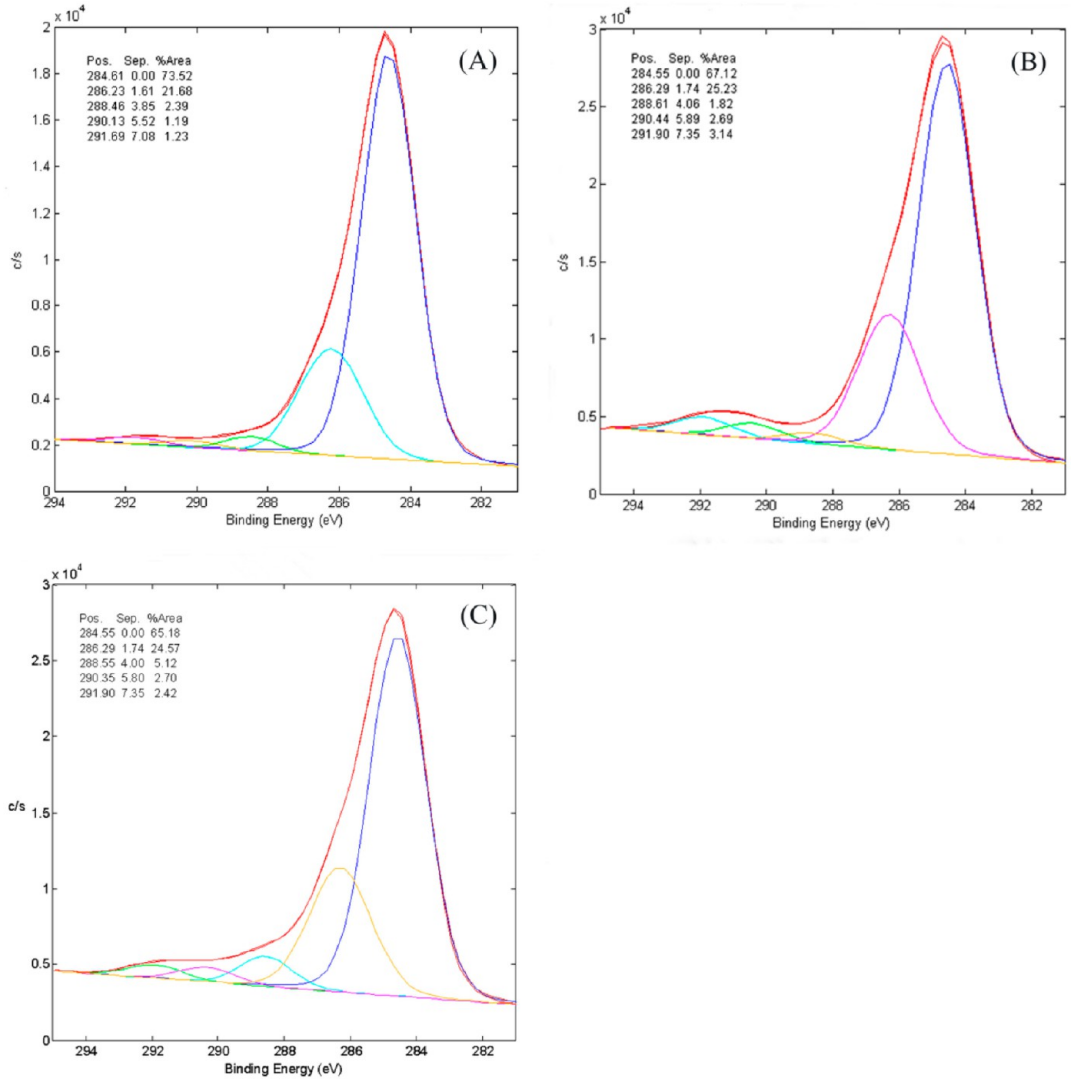

Figure 9. High-resolution C 1s spectra of the samples before swelling (A), after swelling in 18 mol/L H_2SO_4 (B), and after etching in the MnO_2–NaH_2PO_4–H_2SO_4 system (C).

3.4. Sheet Resistance. It has been reported that the SE increased with the decrease in the sheet resistance.[23,24] Figure 13 shows the sheet resistance of the PEEK/MWCNT samples electroless plated for different amounts of time. From Figure 13, the maximum sheet resistance was 10.24 Ω/square (electroless plating for 5 min), and the minimum sheet resistance was 0.88 Ω/square (electroless plating for 40 min). The sheet resistance decreased with the increase of the electroless-plating time. In particular, the values of sheet resistance dropped quickly in the first 20 min, and after that the values dropped slowly. This can be ascribed to the microstructure of the Ni–P coating. As shown in Figure 10C, the Ni–P coating was porous, and Ni–P particles were too small, so the sheet resistance was high (10.24 Ω/square). In Figure10D, as the plating time increased to 10 min, the particles grew so the porosity decreased, and the coating became more compact than that plated for 5 min. Correspondingly, the sheet resistance decreased to 3.41 Ω/square. After 20 min of plating, as shown in Figure 10E, the particles became even larger, and the coating was dense and nonporous, resulting in the sheet resistance dropping to 1.71 Ω/square. After that, the sheet resistance decreased with the increasing thickness of the Ni–P coating, but the reaction became much weaker, and the deposition rate of Ni–P was much slower, resulting in the sheet resistance dropping slowly 20 min later. To overcome this problem, the electroless-plated samples were further coated by electroplating. The sheet resistance of the metalized sample (electroless plating for 20 min followed by electroplating for 20 min) was 0.024 Ω/square. By increasing the electroplating time, the sheet resistance can be reduced further.

3.5. Volume Resistivity. The volume resistivity of the electroless-plated sample was also studied. The PEEK/MWCNT samples were electroless plated for 5, 10, and 30 min. Then, the coatings on four sides were removed by sanding, and only the coatings on the top and the bottom remained. The volume resistivity in the direction of the thickness was measured, as shown in Figure 14. Table 2 shows the volume resistivities of the original PEEK/MWCNT and the electroless-plated PEEK/MWCNT. The volume resistivity of the original PEEK/MWCNT was as high as 2.2×10^4 Ω·m. However, the volume resistivity of the sample electroless plated for 5 min dropped sharply to 38 Ω·m. After that, increasing the plating time had little impact on the volume resistivity. In Figure 3A,

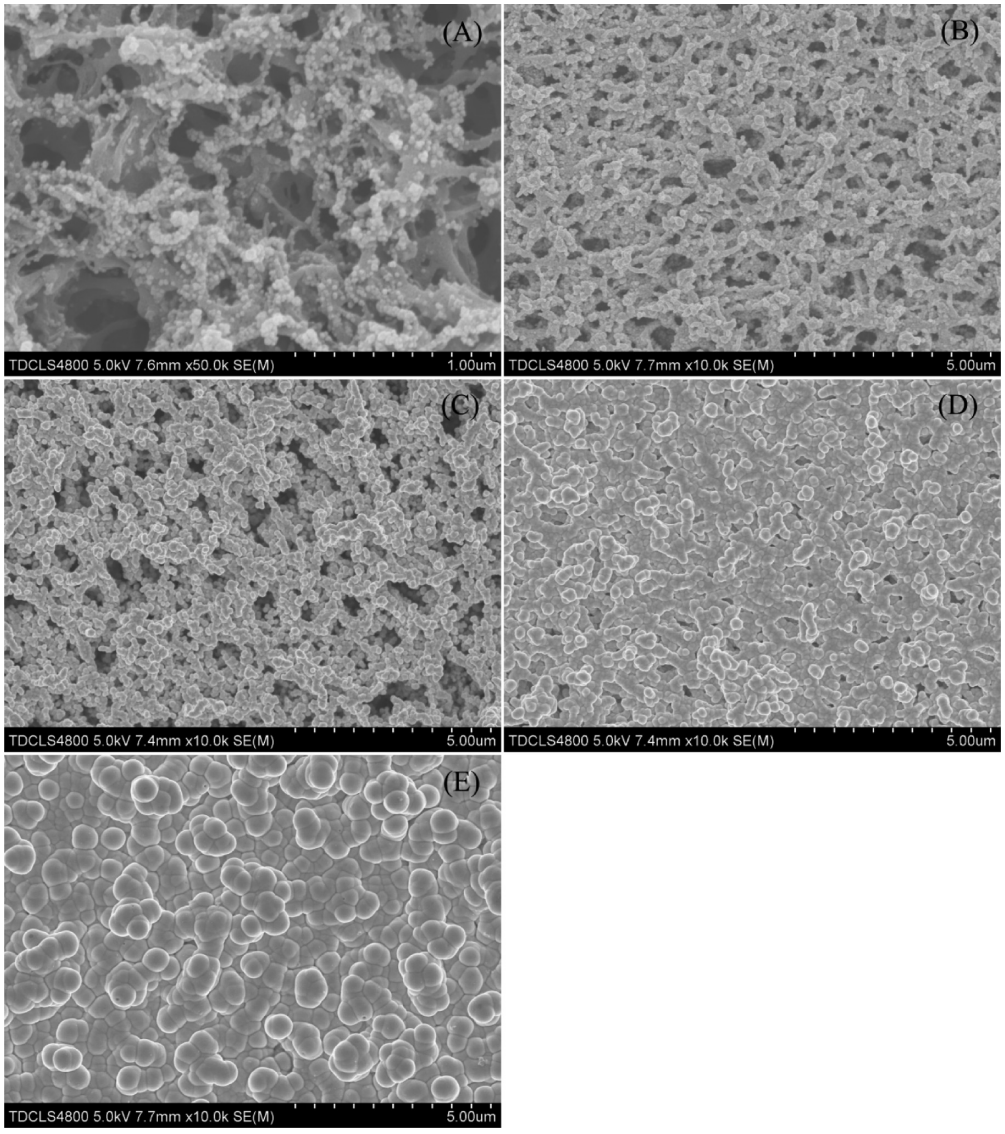

Figure 10. SEM images of the samples after electroless plating for 30 s (A) or for 2 (B), 5 (C), 10 (D), and 20 min (E).

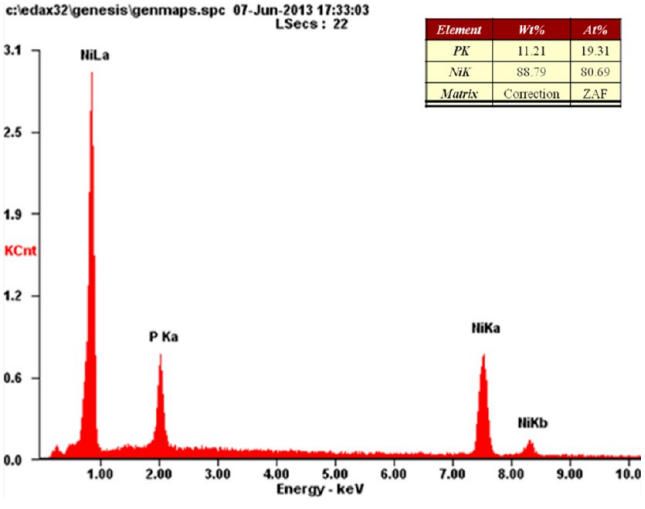

Figure 11. EDX analysis of the Ni–P coating.

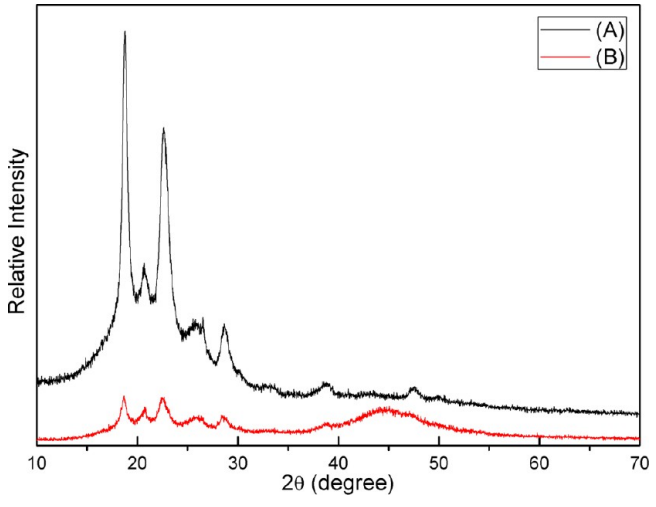

Figure 12. XRD patterns of the surface of PEEK/MWCNT (A) and electroless-plated PEEK/MWCNT (B).

we can see that there was no MWCNT exposed on the surface of PEEK/MWCNT. The MWCNT were wrapped by PEEK,

dx.doi.org/10.1021/am4037806 | ACS Appl. Mater. Interfaces 2013, 5, 12499–12509

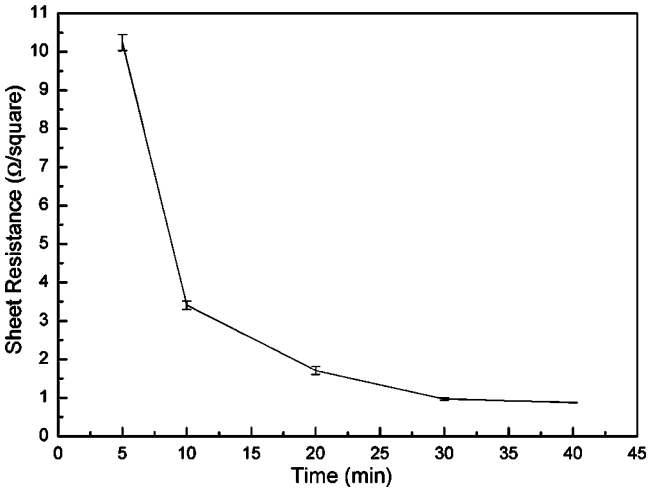

Figure 13. Sheet resistances of the PEEK/MWCNT samples electroless plated for different amounts of time.

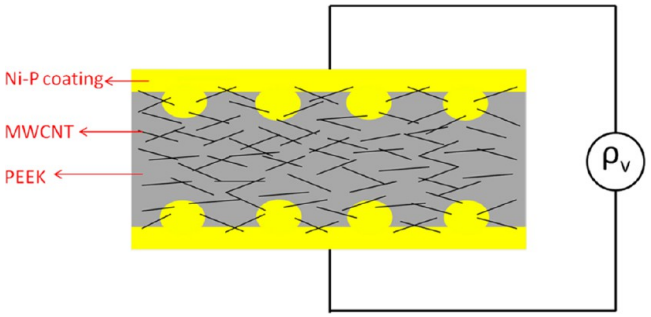

Figure 14. Schematic diagram of the measurement of the two-side-coated sample and the bonding mechanism between the coating and substrate.

which was a highly insulated material, so the volume resistivity of PEEK/MWCNT was high. After etching, as shown in Figure 5C,D, lots of MWCNT were partially exposed on the surface of PEEK/MWCNT samples. The distribution of MWCNT indicated that they entangled and formed a three-dimensional network throughout the matrix. Figure 10A shows that the Ni–P particles deposited on the exposed MWCNT. After plating for 5 min, as shown in Figure 10B, the MWCNT were fully covered by Ni–P particles. Therefore, it seemed likely that the metal coatings on the top and bottom of PEEK/MWCNT were connected by the network of MWCNT, explaining why the volume resistivity of PEEK/MWCNT dropped sharply after electroless plating for 5 min and why increasing the plating time had little effect on it.

3.6. Adhesion. The adhesion of the Ni–P coating (electroless plating for 20 min) was studied by the standard ASTM D3359 Scotch-tape test. After the tape test, none of the squares of the lattice were detached. The adhesion reached the highest scale (5 B) described in ASTM D3359. The test was repeated 20 times on each sample. Even so, none of the squares were removed. The good adhesion is the result of two main factors. First, lots of microscopic holes appeared on the surface after swelling and etching; after electroless plating, the Ni–P coating was embedded in the holes and produced an anchorage effect. Second, lots of MWCNT were partially exposed after etching, and the MWCNT were coated by Ni–P alloy after electroless plating. In other words, for a multiwalled carbon nanotube, one part was embedded in PEEK and another part, in the Ni–P coating; thus, an interaction force between the coating and the PEEK/MWCNT substrate was produced. This can be shown with a schematic diagram (Figure 14).

4. CONCLUSIONS

In this article, we described an environmentally friendly swelling and chemical-etching method to roughen and hydrophilize the surface of PEEK/MWCNT composites, and we then metalized the composites. After the PEEK/MWCNT composites were swelled in 18 mol/L H_2SO_4 for 3 min at room temperature, a high roughness (R_a = 151 nm, R_{ms} = 196 nm) and a small SR (7.1%) were obtained. After etching in the MnO_2–NaH_2PO_4–H_2SO_4 system at 60 °C for 5 min, large numbers of microscopic holes and partially exposed MWCNT were obtained simultaneously, which is needed for reducing the volume resistivity of the PEEK/MWCNT composite and improving the adhesion of the metal coating. Additionally, the percentage of polar groups on the surface was increased, which increased the hydrophilic character of the composite surface. A dense amorphous Ni–P coating was formed after electroless plating for 20 min. The sheet resistance decreased with increasing electroless plating time, and it dropped to 0.88 Ω/square after electroless plating for 40 min. In addition, the volume resistivity of the two-side-plated PEEK/MWCNT dropped sharply to 38 Ω·m after electroless plating for 5 min. The adhesion of the coating reached the highest scale (5 B) described in ASTM D3359, and none of the squares were removed after performing the test 20 times.

AUTHOR INFORMATION

Corresponding Author

*Tel.: +86 13802147382; Fax: +86 022 27404724; E-mail: dayang@tju.edu.cn.

Notes

The authors declare no competing financial interest.

ACKNOWLEDGMENTS

This work is supported by The National Basic Research Program of China (grant no. 2010CB934700) and the National Natural Science Foundation of China (51072130). We thank Professor Yali Li of Tianjin University for his useful suggestions.

REFERENCES

(1) Díez-Pascual, A. M.; Naffakh, M.; González-Domínguez, J. M.; Ansón, A.; Martínez-Rubi, Y.; Martínez, M. T.; Simard, B.; Gómez, M. A. *Carbon* **2010**, *48*, 3500–3511.

Table 2. Volume Resistivities of the Original PEEK/MWCNT and PEEK/MWCNT at Different Amounts of Electroless Plating Time

time (min)	original PEEK/MWCNT	5	10	30
volume resistivity (Ω·m)	$(2.2 \pm 0.1) \times 10^4$	38 ± 0.2	38 ± 0.2	34 ± 0.2

(2) Patel, P.; Stec, A. A.; Hull, T. R.; Naffakh, M.; Diez-Pascual, A. M.; Ellis, G.; Safronava, N.; Lyon, R. E. *Polym. Degrad. Stab.* **2012**, *97*, 2492−2502.
(3) Searle, O. B.; Pfeiffer, R. H. *Polym. Eng. Sci.* **1985**, *25*, 474−476.
(4) Shukla, D.; Negi, Y. S.; Sen Uppadhyaya, J.; Kumar, V. *Polym. Rev.* **2012**, *52*, 189−228.
(5) Diez-Pascual, A. M.; Naffakh, M.; Marco, C.; Ellis, G.; Gomez-Fatou, M. A. *Prog. Mater. Sci.* **2012**, *57*, 1106−1190.
(6) Wang, H. S.; Wang, G. B.; Li, W. L.; Wang, Q. T.; Wei, W.; Jiang, Z. H.; Zhang, S. L. *J. Mater. Chem.* **2012**, *22*, 21232−21237.
(7) Geetha, S.; Kumar, K. K. S.; Rao, C. R. K.; Vijayan, M.; Trivedi, D. C. *J. Appl. Polym. Sci.* **2009**, *112*, 2073−2086.
(8) Domenech, S.; Lima, E., Jr.; Drago, V.; De Lima, J.; Borges, N., Jr.; Avila, A.; Soldi, V. *Appl. Surf. Sci.* **2003**, *220*, 238−250.
(9) Krishnan, K. H.; John, S.; Srinivasan, K. N.; Praveen, J.; Ganesan, M.; Kavimani, P. M. *Metall. Mater. Trans. A* **2006**, *37*, 1917−1926.
(10) Guo, R. H.; Jiang, S. Q.; Yuen, C. W. M.; Ng, M. C. F. *J. Mater. Sci.: Mater. Electron.* **2009**, *20*, 735−740.
(11) Bradley, T.; Schofield, W.; Garrod, R.; Badyal, J. *Langmuir* **2006**, *22*, 7552−7555.
(12) Rytlewski, P.; Żenkiewicz, M.; Tracz, A.; Moraczewski, K.; Mróz, W. *Surf. Coat. Technol.* **2011**, *205*, 5248−5253.
(13) Fristrup, C. J.; Jankova, K.; Hvilsted, S. *Polym. Chem.* **2010**, *1*, 1696−1701.
(14) Bishop, M. T.; Karasz, F. E.; Russo, P. S.; Langley, K. H. *Macromolecules* **1985**, *18*, 86−93.
(15) Hughes, S. W. *Phys. Educ.* **2005**, *40*, 468.
(16) Garcia, A.; Berthelot, T.; Viel, P.; Polesel-Maris, J.; Palacin, S. *ACS Appl. Mater. Interfaces* **2010**, *2*, 3043−3051.
(17) Garcia, A.; Berthelot, T.; Viel, P.; Mesnage, A.; Jégou, P.; Nekelson, F.; Roussel, S.; Palacin, S. *ACS Appl. Mater. Interfaces* **2010**, *2*, 1177−1183.
(18) Wang, Z. L.; Li, Z. X.; He, Y.; Wang, Z. X. *J. Electrochem. Soc.* **2011**, *158*, D664−D670.
(19) Zhao, W. X.; Wang, Z. L. *Int. J. Adhes. Adhes.* **2013**, *41*, 50−56.
(20) Mai, T.; Schultze, J.; Staikov, G. *J. Solid State Electrochem.* **2004**, *8*, 201−208.
(21) Okpalugo, T.; Papakonstantinou, P.; Murphy, H.; McLaughlin, J.; Brown, N. *Carbon* **2005**, *43*, 153−161.
(22) Wang, W. H. *Nat. Mater.* **2012**, *11*, 275−276.
(23) Suzuki, K.; Hashimoto, N.; Oyama, T.; Shimizu, J.; Akao, Y.; Kojima, H. *Thin Solid Films* **1993**, *226*, 104−109.
(24) Lee, H.-C.; Kim, J.-Y.; Noh, C.-H.; Song, K. Y.; Cho, S.-H. *Appl. Surf. Sci.* **2006**, *252*, 2665−2672.